ADVANCED FUNCTIONAL MATERIALS
www.afm-journal.de

Molecularly Imprinted Silver-Halide Reflection Holograms for Label-Free Opto-Chemical Sensing

Yannick Fuchs, Stephanie Kunath, Olivier Soppera, Karsten Haupt, and Andrew G. Mayes**

Hierarchical structuring of materials offers exciting opportunities to construct functional devices that exploit the ordering at different length scales to impart key functional properties. Herein, multiple processes are combined to create complex materials organized at the molecular, nano, and microscales for selective detection of testosterone by label-free opto-chemical sensing. Molecular imprinting is used to construct molecular scale analyte-selective cavities. Microphase separation produces a porous polymer film within which sensitized silver halide nanocolloids are dispersed by a process of infusion and controled precipitation, then converted to periodic layers of silver nanoparticles by holographic patterning followed by chemical development. Testosterone binding is followed via wavelength changes of the holographic reflection peak as a function of testosterone concentration and incubation time. Polymer cross-linking and film porosity are optimized with respect to the needs of both molecular recognition and hologram quality. The silver halide infusion step does not destroy the molecular selectivity of the molecularly imprinted polymers (MIP). Selective, label-free sensing of testosterone is possible at concentrations down to 1 μM. The approach is generic and should be applicable to many types of molecules and conventional MIP formulations, individually or in multiplexed arrays.

1. Introduction

The development of label-free chemical sensors is very attractive for application in industrial, biomedical, environmental, and food analysis. Opto-chemical sensors are of particular interest due to their potentially high sensitivity and easy integration into multisensors for multiplexed read-out, especially if no labeling of the analyte is required. Here, we report for the first time the combination of molecularly imprinted polymers (MIPs) for selective analyte recognition with silver halide holograms for optical signal transduction.

Holographic sensors are a novel, low-cost, and mass-producible family of sensing devices. Their configuration is highly flexible and both transmission and reflection holograms can be used. While a wide range of optical components, such as appearing/disappearing images, can be envisioned, most work to date has focused on simple Bragg reflectors (holograms of plane mirrors), which reflect a narrow band of wavelengths when illuminated with white light. The wavelength of the reflected light λ_{peak} is given by the Bragg equation, where θ is the angle of incidence of the incoming light.

$$\lambda_{peak} = 2\,n\,d\cos\theta \quad (1)$$

The wavelength of the reflected light (λ_{peak}) is dependent on d, the distance between two consecutive holographic layers, and on n, the average refractive index. Changes occurring in the hologram causing modifications of the refractive index and/or d, due to swelling/shrinking, will cause optical changes of the reflected light λ_{peak}, easily detectable instrumentally or even with the naked eye if substantial changes occur. Reflection holograms as sensing devices have already been explored for analytical applications, in different formats such as optical fibers,[1] mesoporous thin films,[2] or combined with a Fabry-Perot filter as a demodulator.[3] In the middle of the 1990s, Lowe's group developed a new approach to label-free sensor fabrication based on silver-halide reflection holograms. These are built from alternating layers (also called fringes) of silver-nanoparticles (AgNPs) obtained by photoreduction of silver-halides stabilized into a gelatin or custom-designed polymer matrix, and acting as Bragg reflectors,[4] and are based on the technology used in photography.[5] When light is absorbed by the silver-halide crystal, it causes local disruption of some of the atomic bonds holding the crystalline structure together freeing some metallic silver atoms within the body of the crystal. Above a certain critical energy, enough silver atoms are released to form a stable speck of metallic silver, also called a latent image.[6] Consequently, only the illuminated areas where the latent image was formed contain metallic silver-clusters. A development step has to be performed to convert the metallic silver crystals into silver grains a few tens of nanometers in diameter. Spatially controled photoreduction is

Dr. Y. Fuchs, Dr. S. Kunath, Prof. K. Haupt
Compiègne University of Technology
CNRS Laboratory Enzyme and Cell Engineering
Rue Roger Couttolenc, CS 60319, 60203
Compiegne Cedex, France
E-mail: karsten.haupt@utc.fr
Dr. O. Soppera
Mulhouse Institute for Material Sciences
CNRS LRC 7228, BP2488, 68057, Mulhouse, France
Dr. A. G. Mayes
University of East Anglia
School of Chemistry
Norwich Research Park
Norwich, NR4 7TJ, UK
E-mail: andrew.mayes@uea.ac.uk

DOI: 10.1002/adfm.201301454

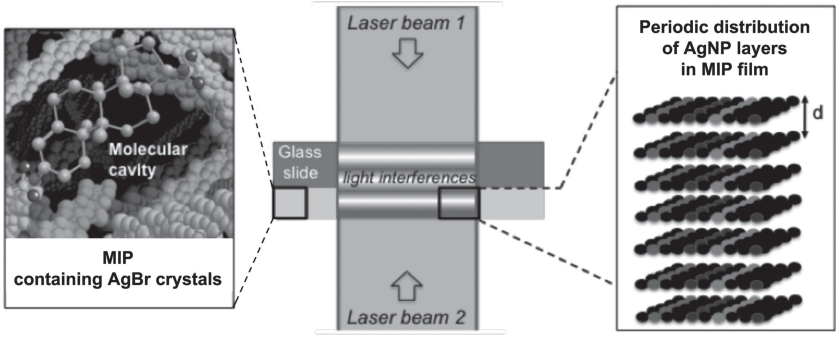

Figure 1. Schematic view of the strategy used to fabricate molecularly imprinted silver-halide reflection holograms. The left part of the figure was reproduced with permission from.[21]

achievable by using a standing wave resulting from interference between two coherent laser beams. Since the first examples of silver-halide holographic sensors developed by Lowe's group,[7] gelatin-stabilized reflection holograms prepared for the detection of different analytes,[4,8] some synthetic polymer hydrogels were also shown to be suitable for the fabrication of analyte-selective silver halide reflection holograms (SHRH),[9–14] though in general it is very challenging to generate hydrogel materials with high levels of analyte specificity. One approach to induce a pronounced analyte specificity in a synthetic polymer is molecular imprinting, and indeed MIPs, also referred to as tailor-made antibody mimics, have been used in opto-chemical sensors.[15,16] MIPs are obtained by a templating process at the molecular level. Polymerization is performed in the presence of functional monomers complexed with a template molecule of interest, driving the formation of a cross-linked polymer network containing cavities that are complementary to the template in terms of size, shape, and position of functional groups. These cavities allow the polymer to bind target analytes with high affinity and specificity.[17,18] The strategy used to develop molecularly imprinted silver-halide reflection holograms (MI-SHRH) is pictured in **Figure 1**, and comprises two steps: first a MIP film is synthesized by using testosterone as a model template,[19,20] and covalently attached to a glass substrate. Afterwards, in a second step, silver bromide (AgBr) is infused into the MIP film with a photosensitizer, and reflection holograms are recorded by passing a collimated 532 nm laser beam through the film backed by a mirror.[6] The resulting layers of silver nanoparticles (AgNPs) periodically distributed within the MIP matrix give rise to a green reflection signal. This can be used for label-free sensing by monitoring MIP film swelling and/or refractive index changes upon molecular recognition and specific binding of testosterone molecules. The key-point of the work presented here was to develop MIP matrices combining molecular specificity, fabrication of SHRH, and structural/optical changes upon analyte binding, thus providing a rapid generic method to build metal colloid-based holograms in MIP materials. Unlike the development of MIP-based transmission holograms recently reported by our group,[21] the route described here is independent of the MIP formulation's properties (monomer viscosity, initiating systems, presence of porogenic solvent) since the MIP film synthesis and the hologram construction are separated. Holograms also show distinct advantages over molecularly imprinted photonic crystals obtained by colloidal templating,[22,23] since they allow the rapid fabrication of macroscale films with homogeneous optical properties over a large surface area and also offer flexibility to produce virtual optical elements and other types of indicators (bar graphs, images etc.) that are useful in visual sensing. The multiscale structuring of MI-SHRH offered by i) the macroscale of the polymer film, ii) the microscale of the polymer pores to provide access to the binding sites, iii) the nanoscale of holographic fringe spacing, and iv) the molecular imprints, make MI-SHRH completely innovative hierarchically-structured functional materials having the potential to give rise to inexpensive, mass-producible label-free sensing devices.

2. Results and Discussion

The optical response of MI-SHRH upon specific molecular binding depends on the efficiency of the molecular imprinting, the polymer flexibility and the accessibility to the binding sites. Therefore, prior to the fabrication of MI-SHRH, the MIP material that would host the holographic element was optimized in bulk format. Testosterone, which is known for its anabolic effects, was chosen as an imprinting target. According to previous studies carried out on testosterone imprinting by self-assembly,[19,20] methacrylic acid (MAA) was chosen as the complexing functional monomer, and ethylene glycol dimethacrylate (EGDMA) as bifunctional cross-linker. The optimal solvent:monomers ratio, providing a good porosity of the polymer network but still yielding a continuous film, was found to be 133%. The challenge of developing a MIP formulation for MI-SHRH lies mainly in providing sufficient freedom to the polymer network to allow subtle changes in the morphology, and hence the volume, of the polymer upon analyte

Table 1. Chemical composition of MIPs S1 to S4, cross-linking density (CLD), uptake capacities (K_{50}) and imprinting factors (IF).

	S1	S2	S3	S4
Testosterone [eq.]	1	1	1	1
MAA [eq.]	8	8	8	8
EGDMA [eq.]	40	24	8	4
DMPA [mol%][a)]	1	1	1	1
Toluene [%][b)]	133	133	133	133
CLD [%][c)]	83	75	50	33
K_{50} [mg mL^{-1}][d)]	0.38	0.34	0.75	N.A.
IF[e)]	5	5	37	17

[a)]The photoinitiator concentration is given in molar percentage of the polymerizable groups in the system; [b)]The solvent concentration is relative to the volume of monomers; [c)] molar ratio of functional monomer to cross-linker; [d)] MIP concentration required to bind the half of the target analyte; [e)] Imprinting factors IF were obtained for a fixed polymer concentration of 0.6 mg mL^{-1} by calculating the ratio of the MIP uptake to the NIP uptake.

binding, while preserving enough network rigidity to maintain the integrity of the MIP binding cavities. The impact of the cross-linking degree on the molecular recognition properties was therefore studied, and four different polymers (S1 to S4) were prepared in bulk format with respectively 83%, 75%, 50%, and 33% of cross-linker relative to the total monomer concentration. However, while decreasing the EGDMA concentration, the molar ratio of MAA to testosterone was kept constant (**Table 1**). Binding experiments performed with the four MIPs in the presence of radiolabeled testosterone showed that the decrease of cross-linking strongly affected the molecular recognition and binding properties of the functional polymer (**Figure 2**). A decrease of cross-linking from 83% (Figure 2A) to 75% (Figure 2B) caused an increase in both specific and non-specific binding, probably due to the simultaneous increase of testosterone and MAA in the system. The imprinting factors (IF = binding to the MIP/binding to the non-imprinted control polymer NIP), however, did not change and the K_{50} (concentration of polymer that binds half of the added radioligand) were similar for both systems, leading to no real improvements. By further decreasing the cross-linking to 50% (Figure 2C), the specific interactions were affected, probably due to the increase in network flexibility, which is assumed to result in a lower imprinting efficiency due to polymer chain mobility, manifested as an increase in K_{50}. However, non-specific interactions between the non-imprinted control polymer (NIP) and testosterone were also strongly decreased, resulting in a higher IF. By cross-linking the MIP at 33% only (Figure 2D), the imprinting effect disappeared, and no K_{50} could be measured. We assume that this level of cross-linking is not sufficient to conserve the integrity of the testosterone specific cavities. The polymer with 50% cross-linking was thus found to be the most suitable for the fabrication of holographic MIP matrices, since it simultaneously allows for moderate polymer film flexibility and specific testosterone recognition and binding.

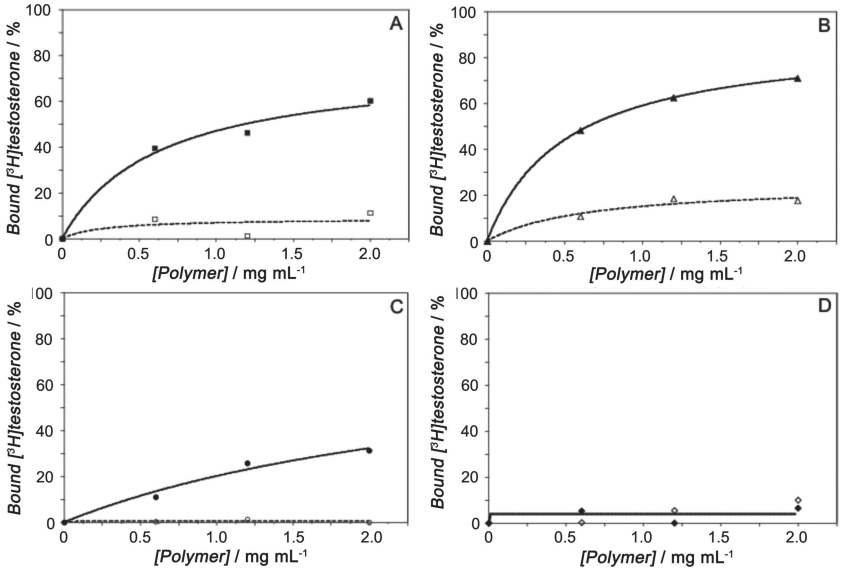

Figure 2. Binding isotherms for radiolabeled testosterone binding in toluene to different MIP (full symbols) and NIP (empty symbols) synthesized in bulk format with different cross-linking degrees: A) 83%, B) 75%, C) 50%, D) 33%.

MIP films were prepared by casting the pre-polymerization mixture between glass substrates and aluminized poly(ethylene terephthalate) (PET) sheets. The glass slides were previously treated with 3-(trimethoxysilyl)propyl methacrylate in order to covalently bond methacrylate groups to the substrate and avoid the peeling of the polymer film after synthesis. 2,2-Dimethoxy-2-phenylacetophenone (DMPA) was employed as UV-photoinitiator,[24] and toluene was used as porogenic solvent to create porosity within the polymer network and favor binding site accessibility. After 30 min of photopolymerization, the PET sheets were taken off, and the films thoroughly washed to extract the molecular template from the MIP and remove the residual chemicals. The films appeared highly diffusing, even when immersed in toluene (**Figure 3**A). Topographic analysis by atomic force microscopy (AFM) revealed macropores with diameters greater than 1 µm, explaining the light scattering effects. A materials-related challenge for the fabrication of MI-SHRH is that the MIP film must be as transparent as possible to allow the laser beam to pass through it (Figure 1), while retaining porosity to give access for the analyte to the binding sites distributed in the film. Depending on the solvent used during polymerization (good or bad solvent for the growing polymer chains), the morphology of the film will vary and result in gel-like transparent materials (good solvent) or opaque macroporous networks (bad solvent), although the refractive index difference between polymer and solvent will also play a role for apparent transparency or opacity. Besides, protic solvents will compete with functional monomers and templates through H-bonding and affect the imprinting efficiency. For the fabrication of MI-SHRH, the dilemma between a homogeneous and transparent film (gel-like) and low resistance to diffusion for access to the binding sites (macroporous) had to be overcome, and different aprotic solvents were compared with toluene. Acetonitrile was finally found to be the best suited solvent to obtain quasi-transparent porous films (Figure 3B). Topographic measurements performed by AFM on an acetonitrile-based film revealed the presence of small pores with diameters below 200 nm. Besides, MIP synthesized in bulk with acetonitrile (with the same composition as polymer S3) showed a smaller K_{50} (0.44 mg mL^{-1} compared to the 0.75 mg mL^{-1}), and higher IFs (78 compared to 38 at a polymer concentration of 0.6 mg mL^{-1}) than the MIP synthesized with toluene, which indicates that acetonitrile is particularly favorable for efficient testosterone imprinting (Supporting Information, Figure SI.1). MIP films were then fabricated with the S3 formulation with acetonitrile as porogen, and their molecular selectivity was studied. Three series of seven films were incubated in acetonitrile with 210 pmol of [4–^{14}C]testosterone, and with increasing concentrations of non-labeled molecular competitors, ranging from 21 pM to 21 mM. The three competitors were i) testosterone, ii) ß-estradiol, which bears a hydroxyl group in C3, as well as a phenyl A-ring, and

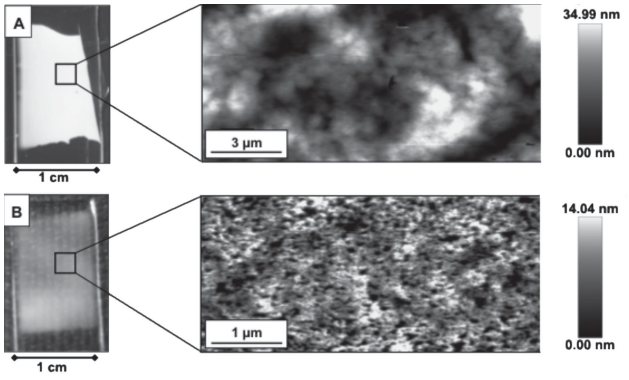

Figure 3. Optical images and surface topography measured by atomic force microscopy (AFM) for polymer films synthesized with A) toluene, or B) with acetonitrile as a porogenic solvent.

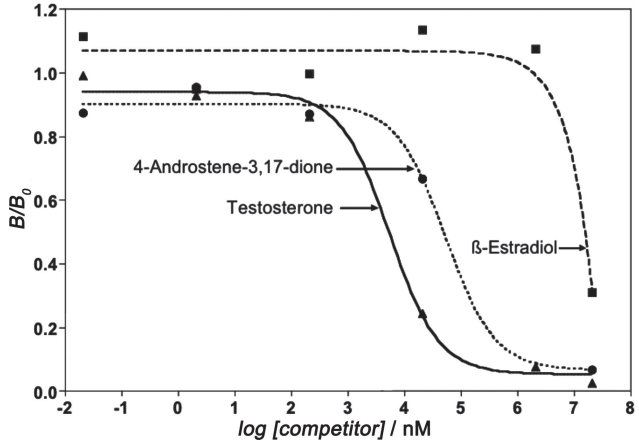

Figure 4. Competitive binding isotherms plotted after incubation of molecularly imprinted films in different steroid solutions containing 210 pmoles of [4–^{14}C]testosterone and increasing concentrations of competitors (testosterone, 4-androstene-3,17-dione, and ß-estradiol). B/B_0 corresponds to the ratio of the signal obtained in the presence of competitor (B) for different concentrations, to the signal measured in the absence of competitor (B_0).

iii) 4-androstene-3,17-dione, which has a keto group at C17 (Supporting Information, Figure SI.2). After 12 h incubation, rinsing and drying, the films were analyzed with a Cyclone phosphorimager, where the presence of radiolabel gave rise to dark coloration (Supporting Information, Figure SI.2). Finally, competitive binding curves could be plotted (**Figure 4**). When testosterone, the imprinting template, was used as a competitor, the binding of [4–^{14}C]testosterone was strongly displaced, and a dissociation constant K_D of 5.4 µM could be determined. When 4-androstene-3,17-dione was present with radiolabeled testosterone, competition was less efficient, resulting in a K_D of 53.8 µM (cross-reactivity of 10%). This may be a consequence of the absence of the C17-hydroxyl group, already reported by Karube's group as dominant in determining the affinity of the substrate for the receptor through H-bonding.[25] ß-estradiol was a poor competitor, showing a cross-reactivity < 0.1%. Owing to the low cross-reactivities experimentally determined with structurally analogues, the MIP films prepared from S3 in acetonitrile showed high specificity and selectivity for testosterone, and were found suitable for use as matrices for the fabrication of silver-halide holographic transducers.

The development of reflection holograms is based on the infusion of silver-halides into the polymeric matrix. The infusion protocol was therefore optimized for the MIP matrix, and performed in two steps. First, silver perchlorate ($AgClO_4$) was dissolved in toluene and infused into the MIP film. Toluene is a reasonable solvent for $AgClO_4$ and also an excellent swelling agent for the MIP, facilitating the infusion process. In a second step, lithium bromide (LiBr) was infused into the silver ion-loaded MIP films to form silver-bromide (AgBr). The LiBr infusion was found to be a critical step for the fabrication of MI-SHRH, since the time had to be tightly controled. An infusion time longer than 30 s resulted in the growth of large silver halide grains, giving rise to a white film in which no hologram could be recorded. After silver-halide infusion, the MIP films were exposed to a 532 nm standing wave to record holograms. The laser power was set to 25 mW, with a spot size of 1 cm, and irradiation times ranging from 5 s to 60 s were tested. It was found that irradiation times longer than 20 s led to overexposure of the film, while 10 s of irradiation was optimal to obtain a bright green-reflecting hologram visible by the naked eye (**Figure 5**A). Sections of MI-SHRH analyzed by scanning electron microscopy (SEM) showed the presence of AgNPs in the polymer film, and confirmed the efficiency of silver-halide photoreduction (Figure 5B,C). The majority of AgNPs are concentrated close to the film surface, presumably as a consequence of the silver and halide ion infusion that is limited by the cross-linked polymer matrix and small pore size. Nevertheless, AgNPs were present in about 60% of the total MIP film thickness (Figure 5B), which was sufficient for recording a strong reflection hologram (Figure 5A). Transmission electron microscopy (TEM) measurements were further performed to observe the distribution of AgNPs in the MIP matrix. Since the MI-SHRH was covalently attached to the glass substrate, its cross-section was difficult to image. The film was therefore scraped off the substrate, and TEM analyzes of the fragments revealed the presence of small AgNPs (diameter < 25 nm) with a narrow size distribution in the polymer matrix (Figure 5D), although the periodic layer structuring was not observable in this way. To verify that the MIP films containing the AgNPs could still bind their target, MIP and NIP silver-halide reflection holograms were incubated with 210 pmoles of [4–^{14}C] testosterone. Analysis using a phosphorimager showed a five times higher binding to the MIP compared to the NIP (Supporting Information, Figure SI.3). This confirmed that the silver-halide fabrication process did not eliminate the specific recognition properties of the MIP.

Prior to analyte sensing experiments, the holographic response to structural changes in the film and the sensor response time were studied. A MI-SHRH was wedged in a spectroscopic cell (polymer face inwards) in such a way as to isolate the holographic reflection peak from the specular reflection (Supporting Information, Figure SI.4). The MI-SHRH was then sequentially incubated in solvents with varying polarity, and

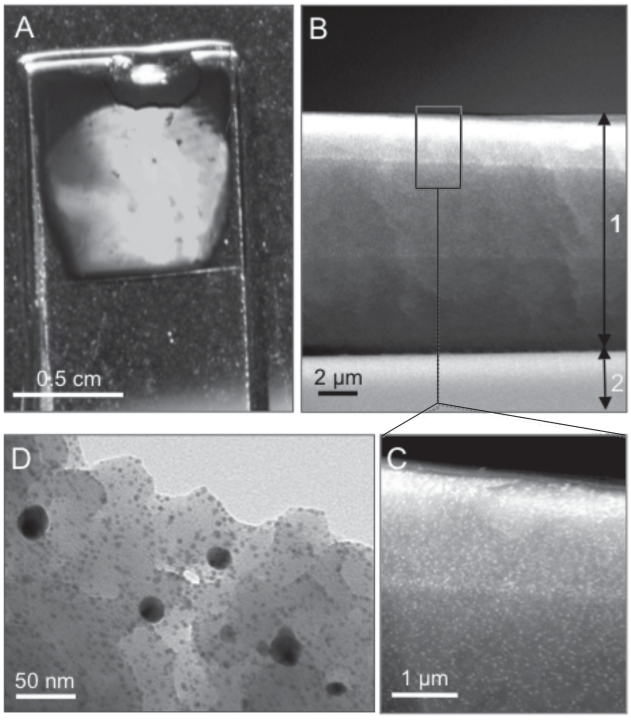

Figure 5. Multiscale characterization of a molecularly imprinted silver-halide reflection hologram. A) Macroscale view of the silver-halide holographic film reflecting green light. B) Microscale view of the section of a MI-SHRH observed using a scanning electron microscope. Zone 1: MIP film; zone 2: glass substrate. C) Zoom into microscale view presented in (B) and showing the presence of AgNPs (white dots) in the polymer film. D) Nanoscale view of a MI-SHRH observed using a transmission electron microscope. Light-grey areas correspond to the MIP and black dots are the AgNPs.

the position of the holographic reflection peak was monitored over time. In order to allow for an accurate measurement of the hologram swelling upon solvent incubation, the MI-SHRH was systematically vacuum dried for 12 h between tests. Incubation of the MI-SHRH in ethanol for 10 h caused a reflection peak shift ($\delta\lambda$) of 2.3 nm, though the optical signal was already stabilized after only 30 min (**Figure 6**A). In the aprotic acetonitrile, the holographic reflection peak was shifted by 5.5 nm, but optical signal stability was reached more slowly (Figure 6B). Increased reflection peak shifts were measured with butyronitrile (Figure 6C) and toluene (Figure 6D), which also increased equilibration time. Taking into account the Bragg equation (Equation 1), non-polar solvents seem to swell better the hydrophobic polymer matrix of the MI-SHRH, resulting in larger increases of the AgNP fringe spacing (d), thus resulting in larger optical shifts of the holographic reflection peak and validating the working principle of this opto-chemical sensor. Although toluene caused more swelling of the polymer films, acetonitrile was employed as incubation medium since it was already used as porogen for the MIP film synthesis.

Subsequent to solvent swelling, a specific volume of testosterone solution was introduced into the spectroscopic cell, and the position of the holographic reflection peak was monitored over time. Testosterone binding assays were conducted with both MI-SHRH and the corresponding non-imprinted control hologram (NI-SHRH), and by using two different testosterone concentrations, 10 µM and 1 µM. After incubation in 10 µM testosterone solution, the MI-SHRH showed a wavelength shift of the reflection peak of $\delta\lambda_{\text{MIP-10}\mu\text{M}} = 3.65$ nm, while the non-imprinted control NI-SHRH gave rise to a wavelength shift of only $\delta\lambda_{\text{NIP-10}\mu\text{M}} = 2.38$ nm. Likewise, after incubation in 1 µM testosterone, the MI-SHRH showed a wavelength shift of $\delta\lambda_{\text{MIP-1}\mu\text{M}} = 2.82$ nm, but the shift with the NI-SHRH was only $\delta\lambda_{\text{NIP-1}\mu\text{M}} = 1.43$ nm. From these results, it is obvious that the wavelength shifts induced in the molecularly imprinted holographic film upon incubation in steroid solutions is bigger than the shifts induced in the non-imprinted holographic films used as control, and confirms the molecular specificity of the MIP matrix, which is capable of taking up testosterone molecules specifically in its binding cavities. Optical changes measured upon binding are, however, relatively small. This may be the consequence of only small structural changes in the polymer matrix upon analyte binding by non-covalent bonds. Nevertheless, the stability of the optical setup employed for the label-free binding assays, and the spectroscopic resolution (0.50 nm for the particular configuration used, which could be increased with more sophisticated signal analysis) still allow for reliable measurements.The holographic sensor response time upon molecular binding was relatively long, which means that 50% cross-linking is still high for this application and limits the polymer film swelling and delays the strain relaxation in the 3D network, which had also been found for MIP-based transmission holographic sensors.[21] Nevertheless, after 8 h of incubation, a good difference between MI-SHRH and NI-SHRH was obtained, resulting in imprinting factors of 18.6 (10 µM testosterone) and of 19.4 (1 µM testosterone).

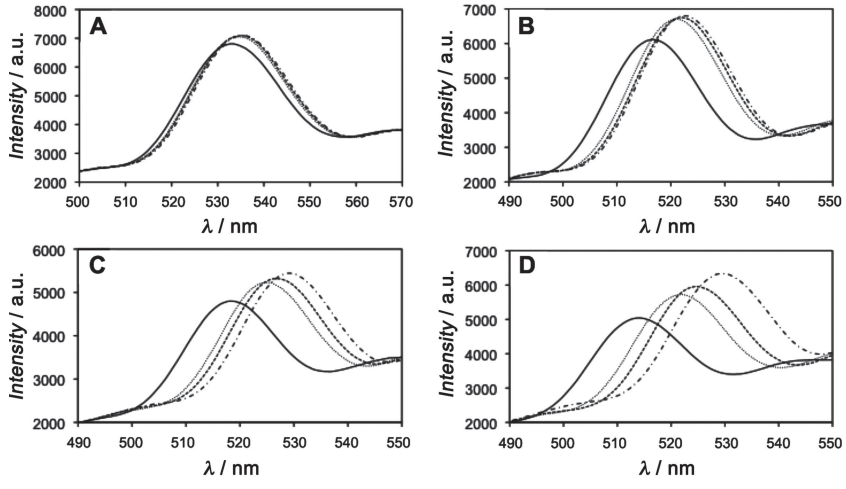

Figure 6. Wavelength position of the reflection peak after incubation of the MI-SHRH in A) ethanol, B) acetonitrile, C) butyronitrile, and D) toluene. Continuous line: $t = 0$, small dashed line: $t = 20$ min, bold dashed line: $t = 1$ h, alternating dashed line: $t = 10$ h).

3. Conclusions

The combination of silver-halide reflection holograms as an optical transducer and molecularly imprinted polymers as recognition elements gave rise to a new type of opto-chemical sensor. MI-SHRH were fabricated in a two-step process, consisting of i) fabricating the MIP film, and ii) creating the holographic element inside the polymer matrix. For the fabrication of the MIP film, the choice of the porogenic solvent was a key parameter to obtain a both transparent and porous film. The fabrication of a silver-halide reflection hologram in the MIP matrix was then achieved by photo- and chemo-reduction of silver halides and chemical fixation of the holographic latent image. This holographic signal was used for label-free binding assays, in which the specific recognition and binding of testosterone molecules to the MIP molecular cavities led to structural changes in the polymer matrix of the holographic element, leading to a wavelength shift of the reflection peak. Specific testosterone recognition and binding could be measured for relatively low analyte concentrations down to 1 µM. We also prepared silver-halide holographic MIP sensors for another target analyte, the beta antagonist (S)-propranolol. Similar results concerning molecular imprinting and sensing properties as with testosterone were obtained (not illustrated). The integration of silver-halide holograms in MIP matrices is highly reproducible and inexpensive, yielding a new type of label-free sensor, and since the integration of silver-halide holograms is possible in any type of MIP film, the method is very versatile and can be applied to sensors for the detection of a large range of analytes including biomolecules such as peptides and proteins.

4. Experimental Section

Materials: Methacrylic acid (MAA), ethylene glycol dimethacrylate (EGDMA), 3-(trimethoxysilyl)propyl methacrylate (TMSPMA, 98%), 2,2-dimethoxy-2-phenylacetophenone (DMPA), testosterone (≥98%) β-estradiol, 4-androstene-3,17-dione, 1,1′-diethyl-2,2′-cyanine iodide, anhydrous silver perchlorate, lithium bromide, hydroquinone, and sodium hydroxide were all purchased from Sigma-Aldrich. Monomers were all used as received, without purification. Sodium thiosulfate pentahydrate was from Merck (Germany). The radiolabelled derivative [1,2,6,7–^{3}H]testosterone (73 Ci mmol^{-1}) was obtained from Amersham Pharmacia Biotech, and [4–^{14}C]testosterone (45–60 mCi mmol^{-1}) was obtained from PerkinElmer. Acetonitrile and toluene were anhydrous and of HPLC grade, and methanol and ethanol were of absolute grade. Water was purified with a RiOs Progard 2 Silver and a Milli-Q Q-Guard 1 system from Millipore (18.2 MΩ cm^{-1}).

Synthesis of Molecularly Imprinted Polymers in Bulk Format: The MIP precursor mixture was placed in a 4 mL transparent glass vial, which was sealed with a septum cap covered with Parafilm, and the mixture was purged with N_2 for 1 min. Polymerization was carried out by placing the vials on a UV light box emitting at 365 nm. After 2 h of irradiation, the polymer was recovered by breaking the glass vial, and the monolith was manually crushed in a mortar. The polymer particles were then transferred to micro-centrifuge tubes, suspended in methanol and finely ground with 2.8 mm-diameter ceramic beads in a Precellys 24 homogenizer (Bertin Technologies, Montigny le Bretonneux, France). The particles were subsequently washed four times using 10 mL of a methanol/acetic acid (9:1 v/v) solution for template extraction, followed by two washes with 10 mL of ethanol and one final wash using 10 mL of methanol. Each washing step was performed for 1 hour in centrifuge tubes under gentle agitation at room temperature. After washing, the particles were separated from the solvent by centrifugation at 25 000 rpm. Finally, the polymer particles were vacuum-dried overnight. The binding assays were performed by suspending increasing concentrations of polymer (ranging from 0 to 9 mg mL^{-1}) in organic solvent (toluene or acetonitrile) in microcentrifuge tubes, and adding 50 µL (0.2 pmoles) of a [1,2,6,7–^{3}H]-testosterone solution at 300 nCi mL^{-1} (final volume of 1 mL[3]). The micro-centrifuge tubes were placed on a rotation wheel overnight. The samples were then centrifuged at 15 000 rpm to sediment the polymer particles. 500 µL of supernatant were subsequently mixed with 3 mL of scintillation liquid (Ultima Gold, PerkinElmer) and ^{3}H counting was performed on a Beckmann LS-6000 IC liquid scintillation counter. The percentage of ^{3}H-labeled testosterone bound to the polymer B(%) relative to the total amount initially introduced could be calculated as follows: $B(\%) = (S_B - S_P)/S_B$, where S_B corresponds to the luminescence intensity of a blank solution including the radiolabeled analyte and the solvent, and S_P to the intensity of the supernatants after incubation of the radiolabeled target analyte with a precise amount of polymer in solution.

Fabrication of Molecularly Imprinted Polymer Films: Microscope glass slides were placed in a ceramic box and incubated for 10 min in a 2.8% aqueous NH_3 solution at 80 °C. The glass slides were then rinsed with water and incubated in a 3% solution of H_2O_2 in H_2O at 80 °C for 10 min. After rinsing with water, the slides were finally incubated for 10 min in a solution containing HCl (37%), H_2O_2 (30%), and H_2O (1 : 1 : 8 v/v/v) at 80 °C. The substrates were rinsed with distilled water and with acetone. The microscope glass slides were then incubated overnight in a solution of 3-(trimethoxysilyl) propyl methacrylate in dry toluene (1 : 90 v/v). Finally, the glass substrates were rinsed several times with acetone, and dried under a stream of nitrogen. MIP films were prepared by casting 3 µL of the freshly made MIP precursor solution on an aluminized polyester film (1 cm × 1 cm), which was then covered with a silanized microscope glass slide (1 cm × 0.5 cm) to form a uniform film. The films were polymerized for 30 min at room temperature by irradiation at 365 nm on a UV light box (VL-6.LC, 4 × 6 W, Fisher Bioblock Scientific). After polymerization, the aluminized polyester was peeled off and the films were rinsed with ethanol. The films were finally washed using the same procedure as described above for bulk polymers. For binding assays the films were placed face-up in 20 mL plastic scintillation vials and covered with 2700 µL of anhydrous solvent. 300 µL (210 pmol) of [4–^{14}C]-testosterone solution at 40 nCi mL^{-1} were then introduced in the plastic vials, and gentle agitation was performed overnight on a rocking table. Afterwards, the films were rinsed for 10 s with the same solvent as the one used for incubation and allowed to dry under ambient conditions. Substrates were placed film side down on a phosphor storage screen for 12 h. The screen was analyzed in a Cyclon Plus system, signal accumulation resulting in dark areas. Subsequent image analysis using ImageJ software[26] allowed the quantification of the radiolabel.

Fabrication of Molecularly Imprinted Silver-Halide Reflection Holograms: Silver halide holograms were recorded in previously fabricated MIP films. The films were first incubated for about 24 h in a silver perchlorate solution prepared in toluene (0.15 M). They were then dried under a gentle stream of warm air from a hair-drier, and soaked for a few seconds in a 0.15 M lithium bromide solution prepared in a mixture of methanol and water (3:1 v/v), containing 140 µM of 1,1′-diethyl-2,2′-cyanine iodide (Sigma) as a photosensitizer. The samples were rinsed with distilled water and placed face down in a holographic exposure bath on a mirror with at an angle of approximately 3° with the help of a glass spacer. The angle of 3° allowed the hologram to be recorded in such a way that the reflected holographic signal was separated from the specular reflection. The film was exposed for a few seconds to the beam of a green laser (doubled Nd:YAG, λ = 532 nm, 50 mW), removed from the exposure bath, and immersed for a few tens of seconds in a freshly prepared developer solution made of sodium hydroxide in water (1.25 M) mixed with hydroquinone in methanol (1.18 M) (1:1 v/v). The film was then thoroughly washed with water, fixed for 10 min under gentle agitation in sodium thiosulfate solution (0.63 M in methanol/water 1:1 v/v), and finally rinsed with distilled water.

Label-Free Sensing with Molecularly Imprinted Silver-Halide Reflection Holograms: Binding assays were performed with silver-halide holographic MIP films placed in an optical setup that enabled the real-time monitoring of the holographic reflection signal. The optical setup included a tungsten-halogen light source emitting in the visible range (300–1050 nm), a fiber optic spectrometer (Ocean optics USB 2000+), and a bifurcated optical fiber assembly. The holographic film was wedged polymer film inwards in a 4 mL quartz cell, and incubated in pure solvent for about 24 h in order to ensure that polymer swelling by the solvent was completed. Afterwards, the target molecule was introduced into the cell, and magnetic stirring was performed. The holographic film was illuminated by a tungsten-halogen source through a Y-shaped optical fiber bundle, and the reflection signal was collected by the same fiber and transmitted to the spectrometer. The initial position of the reflection peak $\lambda_{t=0}$ was recorded after solvent swelling before introduction of the target molecule. Then, the position of the holographic reflection peak was monitored over time, and the wavelength shift $\delta\lambda$ induced by molecular recognition and binding was recorded as a function of the polymer swelling and/or refractive index change. The single pixel resolution enabled measurements of the peak wavelength with a resolution below 0.35 nm to be achieved with this setup, though this can be improved at the expense of wavelength range using spectrometers with different slit and grating options.

Supporting Information

Supporting Information is available from the Wiley Online Library or from the author.

Acknowledgements

The authors gratefully acknowledge the French National Research Agency (Project HOLOSENSE, ANR-08-BLAN-0236–02) for funding. The Regional Council of Picardie and the European Union (CPER 2007–2013), NERC and the Royal Society are acknowledged for funding of equipment.

Received: April 29, 2013
Revised: June 14, 2013
Published online: August 21, 2013

[1] G. Meltz, W. Morey, W. Glenn, *Opt. Lett.* **1989**, *14*, 823.
[2] S. Y. Choi, M. Mamak, G. von Freymann, N. Chopra, G. A. Ozin, *Nano Lett.* **2006**, *6*, 2456.
[3] A. D. Kersey, T. Berkoff, W. Morey, *Opt. Lett.* **1993**, *18*, 1370.
[4] J. Blyth, R. Millington, A. Mayes, E. Frears, C. Lowe, *Anal. Chem.* **1996**, *68*, 1089.
[5] J. Hamilton, *Adv. Phys.* **1988**, *37*, 359.
[6] G. Saxby, in *Practical holography*, 3rd edition, Taylor and Francis, Institute of Physics Publishing, London **2003**.
[7] C. R. Lowe, R. B. Millington, J. Blyth, A. G. Mayes, *EP 1 754 968 A2* **2007**.
[8] R. Millington, A. Mayes, J. Blyth, C. Lowe, *Anal. Chem* **1995**, *67*, 4229.
[9] A. Mayes, J. Blyth, M. Kyrölainen-Reay, R. Millington, C. Lowe, *Anal. Chem* **1999**, *71*, 3390.
[10] A. Mayes, J. Blyth, R. Millington, C. Lowe, *Anal. Chem* **2002**, *74*, 3649.
[11] S. Kabilan, J. Blyth, M. Lee, A. Marshall, A. Hussain, X. Yang, C. Lowe, *J. Mol. Recognit.* **2004**, *17*, 162.
[12] X. Yang, M. C. Lee, F. Sartain, X. Pan, C. R. Lowe, *Chem. Eur. J.* **2006**, *12*, 8491.
[13] A. J. Marshall, J. Blyth, C. A. B. Davidson, C. R. Lowe, *Anal. Chem.* **2003**, *75*, 4423.
[14] A. J. Marshall, D. S. Young, J. Blyth, S. Kabilan, C. R. Lowe, *Anal. Chem.* **2004**, *76*, 1518.
[15] K. Haupt, K. Mosbach, *Chem. Rev* **2000**, *100*, 2495.
[16] O. Y. F. Henry, D. C. Cullen, S. A. Piletsky, *Anal. Bioanal. Chem.* **2005**, *382*, 947.
[17] R. Arshady, K. Mosbach, *Makromol. Chem.* **1981**, *182*, 687.
[18] G. Wulff, A. Sarhan, *Angew. Chem. Int. Ed.* **1972**, *11*, 341.
[19] S. Cheong, S. McNiven, A. Rachkov, R. Levi, K. Yano, I. Karube, *Macromolecules* **1997**, *30*, 1317.
[20] B. T. S. Bui, F. Merlier, K. Haupt, *Anal. Chem.* **2010**, *82*, 4420.
[21] Y. Fuchs, O. Soppera, A. G. Mayes, K. Haupt, *Adv. Mater.* **2012**.
[22] X. Hu, Q. An, G. Li, S. Tao, J. Liu, *Angew. Chem. Int. Ed.* **2006**, *45*, 8145.
[23] Z. Wu, C. Tao, C. Lin, D. Shen, G. Li, *Chem. Eur. J.* **2008**, *14*, 11358.
[24] H. Fischer, R. Baer, R. Hany, I. Verhoolen, M. Walbiner, *J. Chem. Soc., Perkin Trans. 2* **1990**, 787.
[25] S. Cheong, A. Rachkov, J. Park, K. Yano, I. Karube, *J. Polym. Sci., Part A* **1998**, *36*, 1725.
[26] Public domain: http://rsb.info.nih.gov/ij/ (accessed: August 2013).